UNIVERSITÀ DEGLI STUDI DI NAPOLI FEDERICO II
FACOLTÀ DI MEDICINA E CHIRURGIA

DIPARTIMENTO DI MEDICINA CLINICA E SCIENZE CARDIOVASCOLARI ED IMMUNOLOGICHE

DOTTORATO DI RICERCA IN
FISIOPATOLOGIA CLINICA E MEDICINA SPERIMENTALE
Coordinatore: Prof. Gianni Marone

TESI DI DOTTORATO DI RICERCA

THE P2Y$_6$ RECEPTOR INHIBITS EFFECTOR T CELL ACTIVATION IN ALLERGIC PULMONARY INFLAMMATION

TUTOR
Ch.mo Prof. Gianni Marone

DOTTORANDO
Dr. Giorgio Giannattasio

ANNO ACCADEMICO 2009 – 2010

INDEX

INTRODUCTION

Nucleotides, the structural subunits of the nucleic acids, are also important extracellular signaling molecules (Abbracchio and Burnstock, 1998; Burnstock, 2006). They are stored in cytosolic and secretory compartments of cells, and are released in response to cell injury, hypoxia, shear stress, and tissue injury (Bergfeld and Forrester, 1992; Grierson and Meldolesi, 1995; Sprague et al., 1996). Nucleotides are also released in a regulated manner by platelets, endothelial cells, mast cells (MCs), macrophages, and T cells in response to physiologic activation (Milner et al., 1990; Osipchuk and Cahalan, 1992; Smith et al., 2010; Tokunaga et al., 2010). Consequently, extracellular nucleotides accumulate at sites of vascular injury, hypoxia, thrombosis, inflammation, and immune cell activation. Both adenine-containing [adenosine triphosphate (ATP); adenosine diphosphate (ADP)] and uracil-containing [uridine triphosphate (UTP); uridine diphosphate (UDP)] nucleotides have cognate cell surface receptors that mediate their extracellular functions. These receptors fall into two classes; P2X

receptors, which are ligand-gated ion channels that mediate calcium and potassium fluxes in response to ATP, and P2Y receptors, which are G protein-coupled receptors (GPCRs) (Abbracchio et al., 2006; Burnstock and Knight, 2004; Khakh et al., 2001). Although adenine nucleotides and their receptors play established roles in platelet aggregation, pain perception, and cellular responses to hypoxic injury, the functions of many P2Y receptors *in vivo* remain unknown.

$P2Y_6$ receptors are the only known high affinity receptors selective for UDP. They are expressed on both hematopoietic (macrophages, dendritic cells, mast cells, T cells), and nonhematopoietic (vascular smooth muscle, epithelium, endothelium) cell types (Bar et al., 2008; Capra et al., 2005; Chang et al., 1995; Grbic et al., 2008; Jiang et al., 2009; Marcet et al., 2007; Shin et al., 2008; Somers et al., 1998; Southey et al., 1996; Tsukimoto et al., 2009). Most functions attributed to $P2Y_6$ receptors *in vitro* suggest a role in modulating cellular responses to inflammation through autocrine or paracrine actions of uracil nucleotides. Endogenous uracil nucleotides amplify airway

epithelial chemokine production in response to neutrophil-derived peptides through $P2Y_6$ receptors *in vitro* (Khine et al., 2006). $P2Y_6$ receptors are strongly expressed by colonic epithelial cells in biopsies from patients with inflammatory bowel disease, and mediate production of interleukin (IL)-8 by colonic epithelial cell lines *in vitro* (Grbic et al., 2008). $P2Y_6$ receptors amplify chemokine generation by a lipopolysaccharide (LPS)-stimulated monocytic cell line (Warny et al., 2001), and enhance the release of macrophage inflammatory protein-1β by human MCs stimulated with leukotriene D_4 (Jiang et al., 2009). Human T cells express $P2Y_6$ receptors after activation *in vitro* and at sites of inflammation *in vivo* (Somers et al., 1998; Southey et al., 1996), and pharmacologic blockade of $P2Y_6$ receptors inhibits proliferation, CD25 expression, and generation of cytokines by mouse T cells in response to polyclonal and antigen-specific stimulation (Tokunaga et al., 2010; Tsukimoto et al., 2009). Although these *in vitro* studies suggest physiologic functions for $P2Y_6$ receptors in immune responses, such functions have yet to be demonstrated *in vivo*. Given its distribution on cells of both the innate and adaptive

immune systems, we suspected that $P2Y_6$ receptors might play a role in the pathogenesis of allergic pulmonary inflammation. Here, we demonstrate that $P2Y_6$ is an endogenous suppressor of T cell-driven pulmonary pathology induced by exposure to the allergens of the house dust mite *Dermatophagoides farinae*, which are implicated as causative agents in asthma. Newly created C57BL/6 mice bearing a conditional deletion of the $P2Y_6$ receptor [*p2ry6* (flox/flox);cre/+ mice] displayed sharply increased pulmonary inflammation, lymph node hyperplasia, and allergeninduced Th1 and Th2 recall responses compared with $P2Y_6$-sufficient littermate controls [*p2ry6* (flox/flox); (+/+) mice] when exposed intranasally to an extract (*Df*) of *Dermatophagoides farinae*. $P2Y_6$ receptors were constitutively expressed at low levels by alveolar and lung interstitial macrophages, but absent on splenic and parabronchial lymph node (PLN) T cells from naïve mice. However, $P2Y_6$ receptor expression was induced on both CD4+ and CD8+ T cells from PLNs of +/+ mice exposed to *Df*. The absence of $P2Y_6$ receptors from CD4+ T cells of *Df*-challenged mice, but not from lung-derived macrophages used as antigen presenting cells (APCs),

was sufficient to increase Th1 and Th2 cytokine generation in an antigen restimulation assay. Thus, the inducible expression of $P2Y_6$ receptors by T cells permits endogenous UDP to modify cellular activation and cytokine production, thus dampening the lung inflammatory response to the clinically relevant allergens of house dust mites.

MATHERIALS AND METHODS

Generation of +/+ and p2ry6 (flox/flox);cre/+ mice

To generate a viable mouse with a disrupted *p2ry6* gene, we chose a conditional knockout strategy using the established Cre/loxP system. To construct the conditional genetargeting vector, a 12.7 kb region was subcloned from a B6 bacterial artificial chromosome (BAC) clone using homologous recombination (Figure 1A). A single loxP site was inserted at the 5′ side of exon 3 and a PGK-Neo cassette flanked by FRT sites and loxP sites was inserted at the 3′ of exon 3. The region of the targeting vector was designed such that the long (LA) and the short (SA) homology arms extended 9.6 kb at the 5′ side and 2.1 kb at the 3′ of the cassette, respectively. Thus, the target region was ~1.8 kb and included exon 3. The structure of the targeting vector was confirmed by restriction analysis after each modification step and by sequencing using primers designed to read from the selection cassette into the 3′ of the LA (N7) and the 5′ end of the SA (N1) and primers annealing to the vector sequence (P6 and T7) and reading into the 5′ and 3′ ends

of the BAC subclone (Figure 1A). The BAC was subcloned into a 2.4 kb subclone vector containing an ampicillin cassette for retrotransformation of the construct prior to electroporation. The resultant targeting vector was linearized and electroporated into 129/Sv mouse embryonic stem (ES) cells and cells were positively selected with G418. Six verified ES clones were microinjected into blastocysts from C57BL/6 mice and chimeric mice were obtained and crossed with C57BL/6 mice to produce male and female *p2ry6* (flox/+) mice. To generate *p2ry6* (flox/flox) and *p2ry6* (flox/flox);cre/+ mice on a C57BL/6 x 129 mixed background, *p2ry6* (flox/+) mice were intracrossed to produce *p2ry6* (flox/flox) mice. *P2ry6* (flox/flox) mice were then mated with C57BL/6 mice homozygous for the Cre recombinase (cre/cre, C57BL/6 rosa26CreER(T2); TaconicArtemis GmbH, Cologne, Germany) to obtain *p2ry6* (flox/+);cre/+ mice that were then mated with *p2ry6* (flox/flox) mice to produce the experimental mice, *p2ry6* (flox/flox) (+/+ mice) and *p2ry6* (flox/flox);cre/+ (Figure 1B). Once *p2ry6* (flox/flox) and *p2ry6* (flox/flox);cre/+ were obtained, they were also used as breeders for the maintenance of the colony. In order to

generate mice of complete C57BL/6 genetic background, *p2ry6* (flox/+) mice were backcrossed with WT C57BL/6 mice up to the tenth generation (N10). N10 *p2ry6* (flox/+) mice were then mated with cre/cre mice according to the same format described above to finally obtain *p2ry6* (flox/flox) and *p2ry6* (flox/flox);cre/+ mice. In order to induce the Cre recombinase in 5-11 week-old *p2ry6* (flox/flox);cre/+ mice, tamoxifen (1 mg; Sigma), dissolved in a mixture of ethanol/sunflower seed oil (1:4.5, v/v), was injected intraperitoneally daily over 5 consecutive days (Feil et al., 2009). Cohorts of sex- and age-matched *p2ry6* (flox/flox) mice were also administered tamoxifen simultaneously to ensure an equal treatment of the two strains. Tamoxifen-mediated induction of Cre recombinase in *p2ry6* (flox/flox);cre/+ mice resulted in the disruption of *p2ry6* gene (Figures 4 and 8C). Equally treated *p2ry6* (flox/flox) did not show any genetic modification of *p2ry6* gene (Figures 4 and 8C). The mice of the two genotypes were of comparable weight both before the administration of tamoxifen and at beginning of the treatment with *Df* (males: +/+ mice, 25.1 ± 0.3 and 26.7 ± 0.4 g, n = 18; *p2ry6* (flox/flox);cre/+ mice, 25.4 ± 0.3

and 26.1 ± 0.3 g, n = 17; females: +/+, 20.2 ± 0.3 and 21.6 ± 0.2 g, n = 13; *p2ry6* (flox/flox);cre/+, 19.8 ± 0.4 and 21.1 ± 0.6 g, n = 12; from two independent experiments), were indistinguishable clinically and at the histological analysis of lungs, trachea, bone marrow, spleen, liver, stomach, jejunum, colon, kidney, and heart and had similar complete peripheral blood and leukocyte differential count (data not shown).

Mice were genotyped before and after the administration of tamoxifen by semiquantitative PCR of genomic DNA isolated from proteinase K- (from Tritirachium album, Sigma) digested tail samples. Primer sequences were: wild-type *p2ry6*, forward 5'-AGCCTGGTCTACACAGTGAAA-3', reverse 5'-GTAGGGATTCAACATTAGGAG-3'; floxed *p2ry6*, forward 5'-CTTCCTGACTAGGGGAGGAG-3', reverse 5'-GTAGGGATTCAACATTAGGAG-3'; Cre recombinase, forward 5'-CCATCATCGAAGCTTCACTGAAG-3', reverse 5'-GGAGTTTCAATACCCGAGATCATGC-3'.

Mice were housed under specific pathogen-free conditions and maintained on a 12-hour light/dark cycle for the entire duration of

the studies. All the studies described were approved by the Animal Care and Use Committee of the Dana Farber Cancer Institute (Boston, MA).

Df-induced pulmonary inflammation

Ten days after the administration of tamoxifen, pulmonary inflammation was induced in age- (7-13 weeks) and sex-matched +/+ and *p2ry6* (flox/flox);cre/+ mice by intranasal instillation of 3 μg of the *Dermatophagoides farinae* house dust mite extract (*Df*; Greer Laboratories, Lenoir, NC) in 20 μl of NaCl 0.9 % (containing <0.005 EU/ml of endotoxin; Sigma, St. Louis, MO) twice a week for 3 weeks, as described in (Giannattasio et al., 2010; Lundequist et al., 2010). In selected experiments the amount of *Df* was lowered to 1 μg/dose. Control groups of +/+ and *p2ry6* (flox/flox);cre/+ mice received NaCl 0.9% alone. The same protocol was used for the experiments with the cre/+ mice. Twenty-four h after the last treatment, mice were euthanized and blood was collected by cardiac puncture and centrifuged to obtain serum. Mice were then cannulated and bronchoalveolar lavage (BAL) was performed with

three aliquots of 0.7 ml of icecold PBS containing 10% FBS and 0.5 mM EDTA. BAL fluid cells were cytocentrifuged onto slides, stained with Diff-quick (Fisher Diagnostic, Middletown, VA), and differentially counted as mononuclear cells (MNCs, monocytes/macrophages and lymphocytes), neutrophils, or eosinophils, according to the standard hemocytological criteria (Giannattasio et al., 2010).

Histological evaluation of pulmonary inflammation

Left lungs were collected from the mice at the time of euthanasia, fixed for at least 8 h in 4% paraformaldehyde, washed twice with PBS containing 2% DMSO, suspended in 50 mM NH_4Cl overnight at 4°C and finally embedded in paraffin or glycolmethacrylate (Friend et al., 2000). Two-micrometer-thick sections were stained with hematoxylin-azue-2 eosin (H&E) to assess inflammatory cell infiltrates. For histological study of the mucus-secreting cells of the airway epithelia (goblet cells), lung sections were stained with Periodic acid-Schiff (PAS). The extent of cellular infiltration of the tissue was evaluated on fifteen

bronchovascular bundles (BVBs) of comparable large-caliber preterminal bronchi (diameter 200-200 μM) by a pathologist without knowledge of the particular mouse genotype or procedure. The goblet cells positively stained for the presence of mucus at the PAS reaction were enumerated in at least four independent BVBs of each lung and data were expressed as the average of goblet cell counts stained in the bronchi of each section per millimeter of bronchial basal lamina, as measured by Image J (National Institutes of Health image analysis software [http://rsbweb.nih.gov/ij]) (Giannattasio et al., 2010).

Real-time quantitative PCR (qPCR) of mRNA transcripts in the lung and PLNs

Right lungs were collected at time of euthanasia and snap frozen. Freshly isolated PLN cells were pooled from 5-7 mice/group. Total RNA was isolated from tissue homogenates and from PLN cells with Tri-Reagent (Sigma), reverse transcribed into cDNA (RT^2 First Strand kit, SABiosciences, Frederick, MD), and assayed by real-time qPCR for mouse $P2Y_6$, IL-5, IL-13, the

mucus-associated proteins Muc5ac and Clca3/Gob-5, the transcription factors T-bet, GATA-3, and ROR-γT, and GAPDH on a Mx3005P thermal cycler (Stratagene) with the use of SYBR®Green/ROX® master mix (SABiosciences). The ratio of each mRNA relative to the GAPDH mRNA was calculated with the ΔΔCt method. The primers used for mouse $P2Y_6$ (Bar et al., 2008), IL-5, IL-13, Muc5ac, Clca3/Gob-5 and GAPDH were previously reported (Giannattasio et al., 2010). For the transcription factors, the fold-induction was calculated based on the ratio of corrected expression in the samples from *Df*-treated mice and from saline-treated controls.

Immunohistochemical analysis of $P2Y_6$ in lungs, PLNs and spleen

For immunohistochemical analysis of $P2Y_6$ receptors, sections of paraffin-embedded lungs, PLNs and spleens were deparaffinized and rehydrated. Antigen retrieval was performed with Target Retrieval Solution (Dako, Denmark) at 97°C for 30 min. After blocking with 10% chicken serum (Santa Cruz Biotechnologies, Santa Cruz, CA), sections were incubated (1 h, 37ºC) with 43 μg/ml

of a rabbit anti-$P2Y_6$ Ab (Jiang et al., 2009) and then with the peroxidaseconjugated rabbit ABC staining system (Santa Cruz) according to the manufacturer's instructions. Slides were analyzed with a Leica DM LB2 microscope (Leica Microsystems, Wetzlar, Germany) and pictures captured with a Nikon digital camera DXM 1200 with Nikon ACT-1 (version 2.70) image acquisition software.

Flow cytometry analysis of $P2Y_6$ receptors on PLN cells

Pooled PLNs from NaCl- and *Df*-treated +/+ and *p2ry6* (flox/flox);cre/+ mice were homogenized and red cells were lysed. The cells obtained were fixed, permeabilized by incubation in FACS buffer [PBS buffer containing 0.5% bovine serum albumin (Sigma)] + 0.1% saponin (from *Quillaja saponaria*, Sigma) and blocked in FACS buffer containing 10% normal mouse serum and 1% anti-mouse CD16/CD32 (Mouse BD Fc BlockTM, BD Biosciences, San Jose, CA). Cells were washed and incubated (45 min, 4ºC) with the following Abs: allophycocyanin-CD4 (clone RM4-5), allophycocyanin-CD8b (H35-17.2), PE-Cy7-CD11c (N418), PerCP-Cy5.5-B220 (RA3-6B2) (eBioscience), and Alexa

Fluor 488-labeled (Zenon Alexa Fluor 488 rabbit IgG labeling kit, Invitrogen) rabbit anti-$P2Y_6$ [10 μg/ml; (Jiang et al., 2009)]. The corresponding isotypes (eBioscience) or Alexa Fluor 488-labeled normal rabbit IgG (Jackson ImmunoResearch Laboratories) were used as controls. The acquisition was performed on a FACSCanto flow cytometer with FACSDiva software (BD Biosciences), and data were analyzed with FlowJo (Tree Star, Ashland, OR).

In vitro restimulation of lymph node cells with Df

The PLN was collected from the upper-right chest of each mouse and homogenized in complete medium [RPMI, 10% FBS, 1% non-essential amino acids, 2 mM L-glutamine, 100 U/ml penicillin, 100 μg/ml streptomycin, 50 μM 2-ME (Sigma)], plus 25 mM HEPES, and 1 mM sodium pyruvate. The red cells were lysed, and 4 x 10^6 nucleated cells were incubated for 72 h with medium alone or containing 20 μg/ml *Df* (Giannattasio et al., 2010). The concentrations of IL-2, IL-4, IL-5, IL-10, IL-13, IL-17A, and IFN-γ released in the supernatants were measured by ELISA (eBioscience, San Diego, CA). The amount of cytokine per 10^6 PLN cells and the

total number of PLN cells were used to calculate the total amount of cytokine generated per lymph node.

For the ELISPOT analysis, 2.5 x 10^5 PLN nucleated cells were incubated in medium containing *Df* 20 μg/ml for 72 h on 96-well cell culture plates with PVDF filter membranes (Millipore, Billerica, MA), precoated with Abs against IL-4, IL-5, IL-13, IL-17A, and IFN-γ (eBioscience). At the end of the incubation, the cells were removed, the wells washed and spots were detected with an ELISPOT kit (eBioscience) according to the manufacturer's instructions and counted with a CTL Immunospot® Analyzer (Cellular Technology, Shaker Heights, OH). For each cytokine the total number of producing cells was calculated by multiplying the frequency of producing cells by the total number of PLN cells.

Measurement of total and Df-specific serum Igs

Serum from NaCl- and *Df*-treated +/+ and *p2ry6* (flox/flox);cre/+ mice was assayed by ELISA for total IgE content by a commercially available kit (BD Biosciences). *Df*-specific IgG_1 was measured by ELISA with plate-bound *Df*, an alkaline

phosphatase-conjugated anti-mouse IgG_1 (Southern Biotech, Birmingham, AL) and substrate solution (p-nitrophenyl phosphate, Sigma). Absorbance was read at 405 nm, and the results were expressed as net O.D., as described in (Giannattasio et al., 2010).

PLN CD4+ T cell proliferation

PLN cells from NaCl- or *Df*-treated +/+ and *p2ry6* (flox/flox);cre/+ mice were obtained, incubated (10 min, 37ºC) in PBS with 1 μM CFDA-SE (eBioscience) and extensively washed in culture medium. 4 x 10^6 CFDA-SE-labeled cells were then added to 24-well plates precoated with an anti-CD3 Ab (1 μg/ml overnight) and cultured in the presence of soluble anti-CD28 Ab (1 μg/ml) for 72 h. At the end of the incubation cells were harvested, washed in FACS buffer, blocked and incubated (45 min, 4ºC) with APC-CD4 Ab (RM4-5, eBioscience). The acquisition and the analysis were performed as described.

Isolation of lung interstitial macrophages and confocal microscopy

Interstitial macrophages were obtained using a modification of previous protocols (Triggiani et al., 1994; Vermaelen and Pauwels, 2004). After removing airway cells and alveolar macrophages by extensive BAL with PBS containing EDTA, lungs were homogenized through a 70 μm mesh in ice cold complete medium, washed and incubated (30 min, 37ºC) with 428 U/ml Collagenase IV (from Clostridium histolyticum; Worthington, Lakewood, NJ) and 20 μg/ml DNAse I (from bovine pancreas; Roche, Mannheim, Germany). The obtained cell suspension was washed and layered onto a Percoll® gradient (60% and 40%). After centrifugation the cells at each interface were collected, washed, and centrifuged again on a second density gradient. At the end of the procedure the obtained cells, representing an enriched (>85%) population of interstitial macrophages, were stained with Diff-quick (Fisher Diagnostic) or analyzed by flow cytometry with the following antibodies: allophycocianin-CD68 (clone FA-11; AbD Serotec), FITC-MHC-II (M5/114.15.2), PE-Cy7-CD11c, (N418), PE-Cy7-

CD3e (145-2C11), FITC-CD4 (RM4-5), PE-Cy7-CD8a (53-6.7), and PerCP-Cy5.5-B220 (RA3-6B2) (eBioscience).

For confocal microscopy analysis, the macrophages were further enriched by adherence (overnight, 37ºC) on cover slips. After removing non-adherent cells by washing, adherent macrophages were fixed with 2% paraformaldehyde (Sigma) and permeabilized with PBS containing 0.1% saponin (Balestrieri et al., 2009). Cells were incubated (1 h, RT) with goat polyclonal anti-$P2Y_6$ antibody or goat IgG as negative control (10 μg/ml; Santa Cruz). Cells were then incubated (1 h, RT) with FITC-conjugated donkey anti-rabbit IgG (Jackson ImmunoResearch) and pictures were acquired by using a Nikon C1 plus laser scanner confocal system combined with an Eclipse TE2000-U inverted microscope with a x60 oil PlanApo NA 1.4 objective lens. Eight to 10 Z-stack images were acquired and each image (0.5 μm) was saved as a series of independent sections (Balestrieri et al., 2009).

Cocultures of lung macrophages and splenic CD4+ T cells

Interstitial macrophages were obtained as described. To purify CD4+ T cells, spleens of NaCl- or *Df*-treated +/+ and *p2ry6* (flox/flox);cre/+ mice were homogenized and nucleated cells were blocked and incubated (45 min, 4ºC) with PE-Cy7-CD3e (clone 145-2C11) and FITC-CD4 (RM4-5) Abs (eBioscience). The double positive CD3+/CD4+ cells were sorted by flow cytometry (Dana Farber Cancer Institute Flow Cytometry Facility, Boston, MA). Lung interstitial macrophages (1 x 10^5/ml) and CD3+/CD4+ cells (7.5 x 10^5/ml) were cocultured in either medium alone or containing 20 μg/ml *Df* for 72 h. At the end of the incubation the concentrations of IL-5, IL-13, and IFN-γ released in the supernatants were measured by ELISA (eBioscience).

Statistics

Non-parametric Mann-Whitney test and Kruskal-Wallis test with Dunn`s post test correction for multiple comparisons were used to compare two and three or more groups, respectively.

Analysis was performed with Prism software (GraphPad, La Jolla, CA). Values of $p < 0.05$ were considered significant.

RESULTS

Deletion of $P2Y_6$ receptors increases the pulmonary inflammation induced *in vivo* by exposure to *Df* allergen

The *p2ry6* allele was conditionally deleted by flanking the gene with P-lox sites (Figure 1A). The *p2ry6* (flox/flox);cre/+ mice and their +/+ littermate controls were created using the breeding scheme outlined in Figure 1B. The deletion of the *p2ry6* allele was accomplished by the administration of tamoxifen for 5 consecutive days intraperitoneally. PCR analysis was used to confirm the genotype of the mice used in the experiments (Figure 1C). Immunohistochemistry confirmed the absence of the $P2Y_6$ receptor protein in the lungs, PLN and spleen of the *p2ry6* (flox/flox);cre/+ mice after tamoxifen treatment (Figure 4 and data not shown). The initial experiments were performed with F1-F5 C57BL/6 x 129 mice and littermate controls. The results obtained in these experiments were similar to those obtained after backcrossing the mice for 10 generations to the C57BL/6 background (Figures 2A and 2B).

To determine whether $P2Y_6$ receptors played a role in the development of allergic pulmonary inflammation, *Df* (3 μg of protein in 20 μl of NaCl 0.9 %) or saline control was administered intranasally, twice weekly for three consecutive weeks (Lundequist et al., 2010) to cohorts of +/+ and *p2ry6* (flox/flox);cre/+ mice after both genotypes were treated with tamoxifen. Twenty-four hours after the last instillation, mice were euthanized and exsanguinated, BAL was performed and the organs were harvested. Compared with the saline-treated controls, both strains showed significant increases in total BAL fluid cell numbers, eosinophils, neutrophils, macrophages, and lymphocytes when treated with *Df*. However, the total number of cells in BAL fluid of the *Df*-treated *p2ry6* (flox/flox);cre/+ mice exceed that of the +/+ controls by more than 2-fold (Figure 2A). Compared to the *Df*-treated +/+ controls, the *Df*-treated *p2ry6* (flox/flox);cre/+ mice showed ~5-fold higher numbers of BAL fluid eosinophils and neutrophils (Figure 2A). Similar results were obtained after backcrossing the initial F1 mice to the C57BL/6 background for 10 generations (Figure 2B).

To ensure that the activation of the Cre recombinase used to generate the conditional knock-out mouse did not alter the inflammatory response induced by the *Df* in the lung, we treated C57BL/6 *cre/+* mice and WT controls with tamoxifen to activate the Cre recombinase and exposed them to NaCl or *Df* (3 μg) The strains showed essentially identical degrees of *Df*-induced inflammation (Figure 3).

To determine the effect of $P2Y_6$ receptor deficiency on of the development of lung pathology induced by *Df*, we stained the lungs with hematoxylin-azure-2 eosin to identify cellular infiltrates, and by the periodic acid-Schiff reaction to detect goblet cell metaplasia. Because the inflammation caused by *Df* at 3 μg was too severe to show substantial differences between the genotypes (data not shown), we reduced the dose of *Df* to 1 μg in selected experiments to determine whether the deletion of $P2Y_6$ receptors produced an increment in pulmonary inflammation at a lower dose of antigen. At this allergen dose, the bronchovascular bundles (BVBs) of the *p2ry6* (flox/flox);cre/+ mice contained more extensive

inflammatory infiltrates consisting of mononuclear cells along with eosinophils, neutrophils, lymphocytes and plasma cells than did the +/+ controls (Figure 2C). In addition, the bronchial epithelium of the *p2ry6* (flox/flox);cre/+ mice demonstrated more extensive hyperplasia of mucus-producing goblet cells than did the +/+ controls (Figure 2C). Quantitative PCR of the lung RNA revealed higher levels of expression of IL-5 and IL-13 transcripts in the lungs of the *Df*-treated *p2ry6* (flox/flox);cre/+ mice than in the lungs of the +/+ mice, with similar trends for the goblet cell-associated transcripts Muc5ac and Clca3/Gob-5 (Figure 2D).

Cellular distribution of $P2Y_6$ receptors in the lungs and lymphoid tissues

Because the deletion of $P2Y_6$ receptors resulted in increased pulmonary inflammation in response to *Df*, we sought to determine the cellular distribution of $P2Y_6$ receptors in the lungs and associated secondary lymphoid organs of +/+ mice, and whether this distribution and the level of receptor expression changed with the induction of inflammation. qPCR revealed low constitutive

levels of $P2Y_6$ receptor mRNA in the lungs of naïve +/+ mice. These levels sharply increased in response to intranasal *Df* (Figure 4A). Immunohistochemistry of the lungs of saline and *Df*-treated +/+ mice using a rabbit polyclonal anti-$P2Y_6$ antibody (Jiang et al., 2009) revealed that $P2Y_6$ receptor protein localized predominantly to cells with the morphologic appearance of macrophages in the alveolar and interstitial spaces (Figure 4B). Challenge of +/+ mice with *Df* induced the accumulation of mononuclear cells in the bronchus-associated lymphoid tissue of the BVBs, which stained strongly for $P2Y_6$ receptor protein. Based on cell size and morphology, these cells appeared to be a mixture of lymphocytes and monocyte-like cells (Figure 4B). There was negligible staining of the resident epithelial, endothelial, and smooth muscle cells, and no significant staining of the infiltrating granulocytes.

Immunostaining of the spleen and PLNs from naïve +/+ mice revealed negligible staining for $P2Y_6$ receptor protein. In contrast, distinct populations of $P2Y_6$ receptor-positive cells appeared in the paracortical zones of the spleen and PLNs from *Df*-treated +/+ mice (Figure 4C), but not in the germinal centers. Neither the lung

(Figure 4B) nor the lymphoid tissues (Figure 4C) of the saline- or *Df*-treated *p2ry6* (flox/flox);cre/+ mice exhibited staining for $P2Y_6$ receptor protein.

To identify the lymphoid cells inducibly expressing $P2Y_6$ receptors after treatment with *Df*, we performed flow cytometry using the rabbit anti-$P2Y_6$ antibody on the dispersed spleen cells from the +/+ mice. Antibodies against CD4, CD8, B220 (CD45R), and CD11c were used to identify helper and cytotoxic T cells, B cells and APCs, respectively (Figure 5A). No $P2Y_6$-expressing lymphoid cells were identified in the spleens from the naïve +/+ mice (Figure 5B). In contrast, both CD4+ and (to a lesser extent) CD8+ splenic T cells from the *Df*-treated +/+ mice showed modest staining for $P2Y_6$ (Figure 5B). B220+ B cells did not express $P2Y_6$ receptors, whether derived from naïve or *Df*-treated +/+ mice. There were too few CD11c+ cells to analyze, and no staining for $P2Y_6$ receptors was observed on any cell populations in the spleens from saline- or *Df*-treated *p2ry6* (flox/flox);cre/+ mice (Figure 5B). The percentages of CD4+, CD8+, and B220+ cells in the lymph nodes did not differ between the two strains (not shown).

Effects of $P2Y_6$ receptors on the adaptive immune response to *Df*

To determine the role of $P2Y_6$ receptors on control of recall responses to the *Df* antigens in sensitized mice, we evaluated the production of proinflammatory and immunoregulatory cytokines from restimulated PLN cells from the *Df*-treated *p2ry6* (flox/flox);cre/+ mice and +/+ controls. The PLNs from the *Df*-treated *p2ry6* (flox/flox);cre/+ mice were consistently larger than those from the +/+ controls, and contained more total cells (Figure 6A). Equal numbers of PLN cells isolated from NaCl- and *Df*-treated +/+ and *p2ry6* (flox/flox);cre/+ mice were cultured *in vitro* in either medium alone or containing *Df*. At the end of the culture, the concentrations of IL-2, IL-4, IL-5, IL-10, IL-13, IL-17A, and IFN-γ released in the supernatants were evaluated by ELISA. There was no significant cytokine generation by unstimulated cells from either genotype, or by *Df*-stimulated cells from naïve mice (data not shown). Restimulated PLN cells from *Df*-treated *p2ry6* (flox/flox);cre/+ mice generated higher levels of IL-4, IL-5, IL-13,

and IFN-γ than did cells from +/+ mice (Figure 6B). The amounts of IL-2, IL-10 and IL-17A also tended to be higher but did not reach significance. To determine whether the increased quantities of cytokines reflected increased numbers of cytokine-generating cells in the PLNs from *Df*-treated *p2ry6* (flox/flox);cre/+ mice, we performed ELISPOT assays. Consistent with the ELISA data, the PLNs of *Df*-treated *p2ry6* (flox/flox);cre/+ mice contained increased numbers of cells expressing IL-4, IL-5, and IL-13 protein than did the PLNs of the *Df*-treated +/+ controls (Figure 6C). The differences in IFN-γ and IL-17A were not significant.

Quantitative PCR analysis showed that the freshly isolated PLN cells obtained from *Df*-treated *p2ry6* (flox/flox);cre/+ mice exhibited stronger induction (over the PLN cells from corresponding saline-treated controls) of the Th1-associated transcription factor T-bet than did PLN cells from +/+ control mice [7.9-fold induction *vs*. 2.6-fold induction in PLN cells from *Df*-treated *p2ry6* (flox/flox);cre/+ and +/+ mice, respectively; data from 5-7 pooled samples/group]. Similar results were obtained for the Th2-associated transcription factor GATA-3 [5.4-fold induction *vs*.

3.5-fold induction for *p2ry6* (flox/flox);cre/+ and +/+ PLN cells, respectively]. In contrast, the PLN cells from the two strains showed equivalent induction of the regulatory T cell (Treg) associated transcription factor FoxP3 [4.4 *vs*. 4.0-fold induction for *p2ry6* (flox/flox);cre/+ and +/+ PLN cells, respectively]. PLN cells from *p2ry6* (flox/flox);cre/+ mice showed weaker induction of the Th17 transcription factor ROR-γT (0.4 *vs*. 1.1-fold) than did the PLN cells from the +/+ controls (data not shown).

To determine whether the absence of $P2Y_6$ receptors changed the rate of helper T cell proliferation, PLN cells were loaded with CFDA-SE before restimulation and the dilution of the dye was measured cytofluorographically as an index of proliferation. Since the CFDA-SE dilution signal in cultures of PLN cells restimulated with *Df* was below the limit of detection (data not shown), we performed the assay by using a T cell polyclonal stimulation with anti-CD3 and anti-CD28 antibodies. Percentages of proliferating CD4+ T cells were consistently ~10% higher in the PLNs of *p2ry6* (flox/flox);cre/+ mice than in the PLNs of +/+ controls, regardless of whether the samples came from saline-treated or *Df*-treated mice

(54.91 ± 6.52 *vs*. 44.10 ± 4.76 % proliferating CD4+ cells in PLNs of *Df*-treated *p2ry6* (flox/flox);cre/+ *vs*. +/+ controls, respectively, n = 10 mice/group, as shown for one representative mouse per group from one of two experiments, Figure 6D). The *p2ry6* (flox/flox);cre/+ mice exposed to *Df* showed higher levels of serum total IgE (Figure 7A), but they had comparable levels of *Df*-IgG_1 (Figure 7B).

The absence of $P2Y_6$ receptors on CD4+ T cells controls the recall response to *Df*-associated allergens

To determine whether the increased production of cytokines from the restimulated PLNs reflected a direct suppressive effect of $P2Y_6$ receptors expressed by T cells, or an indirect effect of $P2Y_6$ receptor-dependent modulation of APC functions, we developed a co-culture assay. Because there are no available transgenic mice with dust mite allergen-specific T cell receptors, we purified CD3+/CD4+ T cells from the spleens of NaCl- and *Df*-treated +/+ and *p2ry6* (flox/flox);cre/+ mice and incubated them with enriched interstitial macrophages from the lungs of each genotype and

treatment as a source of APCs. After enrichment, nearly all of these cells had morphologic features of macrophages (Figure 8A), with >85% expressing the pan-macrophage marker CD68 (Figure 8B) (Rabinowitz and Gordon, 1991). Less than 5% of the cells expressed T cell markers (CD3, CD4 and CD8); while B220 was expressed by ~15% of the CD68+ cells (data not shown). The proportions of the cells expressing the APC markers CD11c and MHC-II (~40% for each marker) did not differ between genotypes, and confocal imaging confirmed that the macrophages from the *Df*-treated +/+ mice exhibited substantially increased expression of $P2Y_6$ protein relative to the saline-treated controls (Figure 8C). Macrophages from both naïve and *Df*-treated mice were co-cultured with the sorted CD4+ T cells at a fixed ratio in the presence of *Df* for 72 h. CD3+/CD4+ T cells from naïve mice of both genotypes generated small and comparable amounts of IL-5, IL-13 (Figure 9, left panels). In contrast, CD3+/CD4+ T cells from *Df*-treated *p2ry6* (flox/flox);cre/+ mice released more IL-5, IL-13, and IFN-γ than the cells from +/+mice (Figure 9, right panels). There was no effect of the macrophage genotype, although macrophages from lungs of

Df-treated mice supported higher levels of cytokine generation by CD4+ cells than did macrophages from the lungs of saline-treated controls (Figure 9).

DISCUSSION

This study uncovers a prominent role for the UDP-selective $P2Y_6$ receptor in the control of pulmonary inflammation and cytokine generation in a model of allergic pulmonary inflammation. In contrast to the inductive effects of adenine nucleotides (Idzko et al., 2007), which facilitate the development of allergen-induced pulmonary inflammation by breaking tolerance through effects on dendritic cell-associated P2Y receptors, the uracil nucleotides released during this model of pulmonary inflammation act at $P2Y_6$ receptors that are inducibly expressed by T cells to suppress the development of *Df* antigen-responsive T cells and production of pathogenetic cytokines. In this context, the upregulation of $P2Y_6$ receptors on T cells may be a mechanism that limits the pathologic consequences of a pulmonary immune response to allergens that commonly sensitize humans during the development of asthma.

In addition to expression by vascular smooth muscle (Chang et al., 1995), and epithelial cells of the respiratory tract and intestine (Grbic et al., 2008; Marcet et al., 2007), $P2Y_6$ receptors are

expressed by macrophages (Bar et al., 2008; Capra et al., 2005), dendritic cells (Idzko et al., 2004; Shin et al., 2008), T cells (Communi et al., 1996; Somers et al., 1998; Southey et al., 1996; Tokunaga et al., 2010; Tsukimoto et al., 2009), and MCs (Jiang et al., 2009). Although previous studies suggested that $P2Y_6$ receptors primarily serve to amplify cytokine generation by these cells in response to stimuli such as LPS or neutrophil-derived antimicrobial peptides (Khine et al., 2006; Warny et al., 2001), $P2Y_6$ receptor signaling can also suppress certain cellular functions *in vitro* ($CysLT_1R$ signaling, cytokine generation by dendritic cells activated through TLRs) (Capra et al., 2005; Shin et al., 2008) through protein kinase C-dependent mechanisms. There are no previous studies of the role for $P2Y_6$ receptors in an integrated immune response *in vivo*.

We generated a mouse with homozygous floxed *p2ry6* alleles [*p2ry6* (flox/flox)] (Figure 1A) that were disrupted by tamoxifen treatment after introducing a single copy of a tamoxifen-sensitive Cre recombinase allele [*p2ry6* (flox/flox);cre/+] (Figures 1B and 1C). These mice were fertile, healthy, and indistinguishable from

littermate +/+ controls, similar to a previously reported conditional *p2ry6*-/- mice reported in (Bar et al., 2008). We used these mice and their littermates to determine the role of $P2Y_6$ receptors in a model of pulmonary inflammation induced by *Df*, an extract that contains glycans, proteases, and other stimuli that activate lung APCs and initiate a pathogenetic T cell response with the generation of Th1, Th2, and Th17 cytokines and the development of characteristic pulmonary inflammation (Barrett et al., 2009; Giannattasio et al., 2010; Maekawa et al., 2010) when administered intranasally. This model can therefore be used to determine potential contributions from $P2Y_6$ receptors on both the innate and adaptive immune systems to the development of pulmonary pathology. Based on the role for $P2Y_6$ receptors in amplifying cytokine production by immune cells *in vitro*, we anticipated that the deletion of this receptor might reduce inflammation in our model. We were surprised to find that the *p2ry6* (flox/flox);cre/+ mice exhibited increased inflammation after *Df* administration compared with the +/+ littermates, showing significantly increased total cell counts, increased eosinophil and neutrophil counts in the BAL fluid

(Figures 2A and 2B), as well as increased bronchovascular cellular infiltration and goblet cell metaplasia on histological analysis (Figure 2C). The increases in goblet cell-associated transcripts in the lungs of *p2ry6* (flox/flox);cre/+ mice, which are characteristically controlled by the Th2 cytokine IL-13 (Kuperman et al., 2002; Nakanishi et al., 2001; Wills-Karp et al., 1998; Zuhdi Alimam et al., 2000), was paralleled by increased quantities of transcripts encoding IL-13, as well as IL-5, the major cytokine responsible for eosinophilia (Foster et al., 1996; Hogan et al., 1997) (Figure 2D). These data suggested that the absence of $P2Y_6$ receptors increased the expression of pathogenetic Th2 cytokines in the target tissue, leading to characteristic lung pathology.

While cytokine generation in models of allergen-induced pulmonary disease requires T cell activation following the presentation of antigens by APCs (Barrett and Austen, 2009; Barrett et al., 2009; Giannattasio et al., 2010; Trompette et al., 2009), several additional cell types, including epithelial cells, modify cytokine generation by recognizing non-protein components of dust mites (Barrett et al., 2009; Hammad et al., 2009; Trompette et al.,

2009). We therefore sought to determine the distribution and the levels of $P2Y_6$ receptor expression in resident lung cells in both naïve and *Df*-treated mice. Although airway epithelial cells are reported to express $P2Y_6$ receptors, the dominant $P2Y_6$ expressing cells in the lungs of naïve +/+ mice were macrophages in both the alveolar and interstitial spaces of the lung (Figure 4B). The sharply increased expression of $P2Y_6$ receptor transcript in the lungs of *Df*-treated +/+ mice (Figure 4A) was paralleled by the appearance of monocytoid and lymphocytoid cells that strongly expressed $P2Y_6$ receptor protein, and that localized to the bronchus-associated lymphoid tissues (Figure 4B). Additionally, staining of the regional lymph nodes and of the spleen suggested that *Df* treatment of +/+ mice induced a $P2Y_6$ receptor-expressing T cell population (Figure 4C), and flow cytometry verified that PLN CD4+ cells (and, to a lesser extent, CD8+ cells) expressed $P2Y_6$ receptors after exposure *in vivo* to allergen (Figure 5). Moreover, the absence of $P2Y_6$ receptor expression on B220+ B cells is consistent with the lack of immunostaining of germinal centers (Figure 4C). Because the numbers of CD11c+ APCs in the PLNs were very small, we were

unable to determine whether they expressed $P2Y_6$ receptors, although APCs enriched from the lung did express $P2Y_6$ receptors that were upregulated with *Df* treatment (Figures 8B and 8C).

To evaluate the functions of $P2Y_6$ receptors on the secondary lymphoid organs, we next sought to determine the effects of $P2Y_6$ receptor deletion on the recall response to antigen. The PLNs from the *Df*-treated *p2ry6* (flox/flox);cre/+ mice contained more total cells (Figure 6A) than did the PLNs from the +/+ controls. Although the total percentages of T cells in the PLNs did not differ between the strains (data not shown), the restimulated PLN cells from the *Df*-treated *p2ry6* (flox/flox);cre/+ mice generated significantly higher amounts of Th1 and Th2 cytokines than did samples from the +/+ mice (Figure 6B), paralleled by higher numbers of cytokine producing T cells (Figure 6C). Combined with the stronger induction of both T-bet and GATA-3 in the PLNs from *p2ry6* (flox/flox);cre/+ mice than in the PLNs from +/+ controls, the data argue that the effect of $P2Y_6$ receptors on the control of antigen recall responses is not restricted to one lineage of effector T cell. Moreover, the robust generation of IL-10 (Figure 6B) by the

samples from *p2ry6* (flox/flox);cre/+ mice, and the induction of comparable levels of the mRNA encoding Foxp3 in PLN cells from +/+ and *p2ry6* (flox/flox);cre/+ mice following exposure to *Df* suggest that the absence of $P2Y_6$ does not impair induction of regulatory T cells as a mechanism to account for the increased *Df*-induced inflammatory response. Our data argue that $P2Y_6$ receptors, induced by antigen stimulation, play a homeostatic role in the control of memory T cell activation during recall responses. The modest increment in proliferation observed in the polyclonally stimulated CD4+ PLN T cells from *p2ry6* (flox/flox);cre/+ mice compared with +/+ control cells is also consistent with a homeostatic role for $P2Y_6$, although proof of such a role in control of antigen induced proliferation awaits the creation of transgenic mice with T cell receptors specific for *Df* antigens.

In addition to intrinsic properties of the responder T cells, factors that regulate the phenotype of APCs can strongly influence the magnitude and nature of antigen-induced recall responses (Barrett and Austen, 2009; Barrett et al., 2009; Giannattasio et al., 2010; Trompette et al., 2009). To test whether expression of $P2Y_6$

receptors by APCs, by effector T cells, or by both cell types was relevant to the outcome of the *Df*-induced recall response, we developed a crossover assay in which purified $P2Y_6$ receptor-deficient or -sufficient splenic CD4+ T cells were co-cultured with either $P2Y_6$ receptor-deficient or -sufficient lung interstitial macrophages as a source of $P2Y_6$-expressing APCs (Figures 4B and 8C) (Hume, 2008). The induction of inflammation by *Df* causes APCs to mature and become more effective in processing and presenting antigen, likely explaining the ability of the CD4+ cells to produce higher level of cytokines when co-cultured with APC that were derived from *Df*-treated mice. The absence of $P2Y_6$ receptors from the lung macrophages did not affect the expression of activated APC markers CD11c and MHC-II (Figure 8B). Moreover, the macrophage genotype had no influence on the levels of cytokines generated by responder T cells, whereas the CD4+ cells from the *Df*-treated *p2ry6* (flox/flox);cre/+ mice generated more IL-5, IL-13, and IFN-γ than did the CD4+ T cells from the +/+ controls (Figure 9). Thus, at least at the effector phase of the *Df*-induced immune response, the upregulation of $P2Y_6$ on *Df*-treated CD4+

cells is both necessary and sufficient to dampen the production of cytokines in response to stimulation with the allergen in a recall response, suggesting that $P2Y_6$ receptors intrinsically control T cell activation in response to antigen.

Our study demonstrates the first homeostatic role of $P2Y_6$ receptors in the intrinsic control of effector T cell responses to clinically relevant allergens. The findings indicate a $P2Y_6$ receptor-dependent suppressive function for the uracil nucleotides that are generated in the inflammatory milieu during exposure to dust mite allergens. Two recent studies reported that uridine, the precursor of UDP and UTP, has a protective function in two models of acute lung inflammation by acting on epithelial cells (Evaldsson et al., 2007; Müller et al., 2010). Thus, uracil and its derivatives may suppress allergic pulmonary inflammation by several mechanisms, contrasting with the proinflammatory effects of adenine nucleotides in a similar context. Given the multitude of P2Y receptors that are expressed by cells of the immune system, it is critical to understand both the pro- and anti-inflammatory effects of any P2Y receptor

that is envisioned as a potential target for drug development in the treatment of inflammatory diseases.

REFERENCES

Abbracchio, M.P., and Burnstock, G. (1998). Purinergic signaling: pathophysiological roles. Jpn J Pharmacol 78, 113-145.

Abbracchio, M.P., Burnstock, G., Boeynaems, J.M., Barnard, E.A., Boyer, J.L., Kennedy, C., Knight, G.E., Fumagalli, M., Gachet, C., Jacobson, K.A., and Weisman, G.A. (2006). International Union of Pharmacology LVIII: update on the P2Y G protein-coupled nucleotide receptors: from molecular mechanisms and pathophysiology to therapy. Pharmacol Rev 58, 281-341.

Balestrieri, B., Maekawa, A., Xing, W., Gelb, M.H., Katz, H.R., and Arm, J.P. (2009). Group V secretory phospholipase A_2 modulates phagosome maturation and regulates the innate immune response against Candida albicans. J Immunol 182, 4891-4898.

Bar, I., Guns, P.J., Metallo, J., Cammarata, D., Wilkin, F., Boeynams, J.M., Bult, H., and Robaye, B. (2008). Knockout mice reveal a role for $P2Y_6$ receptor in macrophages,

endothelial cells, and vascular smooth muscle cells. Mol Pharmacol 74, 777-784.

Barrett, N.A., and Austen, K.F. (2009). Innate cells and T helper 2 cell immunity in airway inflammation. Immunity 31, 425-437.

Barrett, N.A., Maekawa, A., Rahman, O.M., Austen, K.F., and Kanaoka, Y. (2009). Dectin-2 recognition of house dust mite triggers cysteinyl leukotriene generation by dendritic cells. J Immunol 182, 1119-1128.

Bergfeld, G.R., and Forrester, T. (1992). Release of ATP from human erythrocytes in response to a brief period of hypoxia and hypercapnia. Cardiovasc Res 26, 40-47.

Burnstock, G. (2006). Pathophysiology and therapeutic potential of purinergic signaling. Pharmacol Rev 58, 58-86.

Burnstock, G., and Knight, G.E. (2004). Cellular distribution and functions of P2 receptor subtypes in different systems. Int Rev Cytol 240, 31-304.

Capra, V., Ravasi, S., Accomazzo, M.R., Citro, S., Grimoldi, M., Abbracchio, M.P., and Rovati, G.E. (2005). $CysLT_1$ receptor

is a target for extracellular nucleotide-induced heterologous desensitization: a possible feedback mechanism in inflammation. J Cell Sci 118, 5625-5636.

Chang, K., Hanaoka, K., Kumada, M., and Takuwa, Y. (1995). Molecular cloning and functional analysis of a novel P2 nucleotide receptor. J Biol Chem 270, 26152-26158.

Communi, D., Parmentier, M., and Boeynaems, J.M. (1996). Cloning, functional expression and tissue distribution of the human $P2Y_6$ receptor. Biochem Biophys Res Commun 222, 303-308.

Evaldsson, C., Ryden, I., and Uppugunduri, S. (2007). Anti-inflammatory effects of exogenous uridine in an animal model of lung inflammation. Int Immunopharmacol 7, 1025-1032.

Feil, S., Valtcheva, N., and Feil, R. (2009). Inducible Cre mice. Methods Mol Biol 530, 343-363.

Foster, P.S., Hogan, S.P., Ramsay, A.J., Matthaei, K.I., and Young, I.G. (1996). Interleukin 5 deficiency abolishes eosinophilia,

airways hyperreactivity, and lung damage in a mouse asthma model. J Exp Med 183, 195-201.

Friend, D.S., Gurish, M.F., Austen, K.F., Hunt, J., and Stevens, R.L. (2000). Senescent jejunal mast cells and eosinophils in the mouse preferentially translocate to the spleen and draining lymph node, respectively, during the recovery phase of helminth infection. J Immunol 165, 344-352.

Giannattasio, G., Fujioka, D., Xing, W., Katz, H.R., Boyce, J.A., and Balestrieri, B. (2010). Group V secretory phospholipase A_2 reveals its role in house dust mite-induced allergic pulmonary inflammation by regulation of dendritic cell function. J Immunol 185, 4430-4438.

Grbic, D.M., Degagne, E., Langlois, C., Dupuis, A.A., and Gendron, F.P. (2008). Intestinal inflammation increases the expression of the $P2Y_6$ receptor on epithelial cells and the release of CXC chemokine ligand 8 by UDP. J Immunol 180, 2659-2668.

Grierson, J.P., and Meldolesi, J. (1995). Shear stress-induced [Ca2+]i transients and oscillations in mouse fibroblasts are

mediated by endogenously released ATP. J Biol Chem 270, 4451-4456.

Hammad, H., Chieppa, M., Perros, F., Willart, M.A., Germain, R.N., and Lambrecht, B.N. (2009). House dust mite allergen induces asthma via Toll-like receptor 4 triggering of airway structural cells. Nat Med 15, 410-416.

Hogan, S.P., Mould, A., Kikutani, H., Ramsay, A.J., and Foster, P.S. (1997). Aeroallergen-induced eosinophilic inflammation, lung damage, and airways hyperreactivity in mice can occur independently of IL-4 and allergen-specific immunoglobulins. J Clin Invest 99, 1329-1339.

Hume, D.A. (2008). Macrophages as APC and the dendritic cell myth. J Immunol 181, 5829-5835.

Idzko, M., Hammad, H., van Nimwegen, M., Kool, M., Willart, M.A., Muskens, F., Hoogsteden, H.C., Luttmann, W., Ferrari, D., Di Virgilio, F., et al. (2007). Extracellular ATP triggers and maintains asthmatic airway inflammation by activating dendritic cells. Nat Med 13, 913-919.

Idzko, M., Panther, E., Sorichter, S., Herouy, Y., Berod, L., Geissler, M., Mockenhaupt, M., Elsner, P., Girolomoni, G., and Norgauer, J. (2004). Characterization of the biological activities of uridine diphosphate in human dendritic cells: Influence on chemotaxis and CXCL8 release. J Cell Physiol 201, 286-293.

Jiang, Y., Borrelli, L., Bacskai, B.J., Kanaoka, Y., and Boyce, J.A. (2009). $P2Y_6$ receptors require an intact cysteinyl leukotriene synthetic and signaling system to induce survival and activation of mast cells. J Immunol 182, 1129-1137.

Khakh, B.S., Burnstock, G., Kennedy, C., King, B.F., North, R.A., Seguela, P., Voigt, M., and Humphrey, P.P. (2001). International union of pharmacology. XXIV. Current status of the nomenclature and properties of P2X receptors and their subunits. Pharmacol Rev 53, 107-118.

Khine, A.A., Del Sorbo, L., Vaschetto, R., Voglis, S., Tullis, E., Slutsky, A.S., Downey, G.P., and Zhang, H. (2006). Human neutrophil peptides induce interleukin-8 production through the $P2Y_6$ signaling pathway. Blood 107, 2936-2942.

Kuperman, D.A., Huang, X., Koth, L.L., Chang, G.H., Dolganov, G.M., Zhu, Z., Elias, J.A., Sheppard, D., and Erle, D.J. (2002). Direct effects of interleukin-13 on epithelial cells cause airway hyperreactivity and mucus overproduction in asthma. Nat Med 8, 885-889.

Lundequist, A., Nallamshetty, S.N., Xing, W., Feng, C., Laidlaw, T.M., Uematsu, S., Akira, S., and Boyce, J.A. (2010). Prostaglandin E_2 exerts homeostatic regulation of pulmonary vascular remodeling in allergic airway inflammation. J Immunol 184, 433-441.

Maekawa, A., Xing, W., Austen, K.F., and Kanaoka, Y. (2010). GPR17 regulates immune pulmonary inflammation induced by house dust mites. J Immunol 185, 1846-1854.

Marcet, B., Horckmans, M., Libert, F., Hassid, S., Boeynaems, J.M., and Communi, D. (2007). Extracellular nucleotides regulate CCL20 release from human primary airway epithelial cells, monocytes and monocyte-derived dendritic cells. J Cell Physiol 211, 716-727.

Milner, P., Bodin, P., Loesch, A., and Burnstock, G. (1990). Rapid release of endothelin and ATP from isolated aortic endothelial cells exposed to increased flow. Biochem Biophys Res Commun 170, 649-656.

Müller, T., Grimm, M., de Vieira, R.P., Cicko, S., Dürk, T., Sorichter, S., Zissel, G., and Idzko, M. (2010). Local administration of uridine suppresses the cardinal features of asthmatic airway inflammation. Clin Exp Allergy 40, 1552-1560.

Nakanishi, A., Morita, S., Iwashita, H., Sagiya, Y., Ashida, Y., Shirafuji, H., Fujisawa, Y., Nishimura, O., and Fujino, M. (2001). Role of gob-5 in mucus overproduction and airway hyperresponsiveness in asthma. Proc Natl Acad Sci U S A 98, 5175-5180.

Osipchuk, Y., and Cahalan, M. (1992). Cell-to-cell spread of calcium signals mediated by ATP receptors in mast cells. Nature 359, 241-244.

Rabinowitz, S.S., and Gordon, S. (1991). Macrosialin, a macrophage-restricted membrane sialoprotein differentially

glycosylated in response to inflammatory stimuli. J Exp Med 174, 827-836.

Shin, A., Toy, T., Rothenfusser, S., Robson, N., Vorac, J., Dauer, M., Stuplich, M., Endres, S., Cebon, J., Maraskovsky, E., and Schnurr, M. (2008). P2Y receptor signaling regulates phenotype and IFN-alpha secretion of human plasmacytoid dendritic cells. Blood 111, 3062-3069.

Smith, J.P., Haddad, E.V., Downey, J.D., Breyer, R.M., and Boutaud, O. (2010). PGE_2 decreases reactivity of human platelets by activating EP_2 and EP_4. Thromb Res 126, e23-29.

Somers, G.R., Hammet, F.M., Trute, L., Southey, M.C., and Venter, D.J. (1998). Expression of the $P2Y_6$ purinergic receptor in human T cells infiltrating inflammatory bowel disease. Lab Invest 78, 1375-1383.

Southey, M.C., Hammet, F., Hutchins, A.M., Paidhungat, M., Somers, G.R., and Venter, D.J. (1996). Molecular cloning and sequencing of a novel human P2 nucleotide receptor. Biochim Biophys Acta 1309, 77-80.

Sprague, R.S., Ellsworth, M.L., Stephenson, A.H., and Lonigro, A.J. (1996). ATP: the red blood cell link to NO and local control of the pulmonary circulation. Am J Physiol 271, H2717-2722.

Tokunaga, A., Tsukimoto, M., Harada, H., Moriyama, Y., and Kojima, S. (2010). Involvement of SLC17A9-dependent vesicular exocytosis in the mechanism of ATP release during T cell activation. J Biol Chem.

Triggiani, M., Oriente, A., and Marone, G. (1994). Differential roles for triglyceride and phospholipid pools of arachidonic acid in human lung macrophages. J Immunol 152, 1394-1403.

Trompette, A., Divanovic, S., Visintin, A., Blanchard, C., Hegde, R.S., Madan, R., Thorne, P.S., Wills-Karp, M., Gioannini, T.L., Weiss, J.P., and Karp, C.L. (2009). Allergenicity resulting from functional mimicry of a Toll-like receptor complex protein. Nature 457, 585-588.

Tsukimoto, M., Tokunaga, A., Harada, H., and Kojima, S. (2009). Blockade of murine T cell activation by antagonists of $P2Y_6$

and $P2X_7$ receptors. Biochem Biophys Res Commun 384, 512-518.

Vermaelen, K., and Pauwels, R. (2004). Accurate and simple discrimination of mouse pulmonary dendritic cell and macrophage populations by flow cytometry: methodology and new insights. Cytometry A 61, 170-177.

Warny, M., Aboudola, S., Robson, S.C., Sevigny, J., Communi, D., Soltoff, S.P., and Kelly, C.P. (2001). P2Y(6) nucleotide receptor mediates monocyte interleukin-8 production in response to UDP or lipopolysaccharide. J Biol Chem 276, 26051-26056.

Wills-Karp, M., Luyimbazi, J., Xu, X., Schofield, B., Neben, T.Y., Karp, C.L., and Donaldson, D.D. (1998). Interleukin-13: central mediator of allergic asthma. Science 282, 2258-2261.

Zuhdi Alimam, M., Piazza, F.M., Selby, D.M., Letwin, N., Huang, L., and Rose, M.C. (2000). Muc-5/5ac mucin messenger RNA and protein expression is a marker of goblet cell metaplasia in murine airways. Am J Respir Cell Mol Biol 22, 253-260.

Figure Legends

Figure 1. Generation of +/+ and *p2ry6* (flox/flox);cre/+ mice

(A) The conditional gene-targeting vector was obtained from an ~12.7 kb B6 bacterial artificial chromosome subclone and contained a long homology arm (LA; 9.6 kb), *p2ry6* exons 2 and 3, the latter flanked at the 5′ side by a single loxP site and at the 3′ side by a PKG-neo cassette with loxP and FRT sites, and a short homology arm (SA; 2.1 kb). The target region was ~1.8 kb and included exon 3. The annealing sites of the primers used to confirm the structure of the vector are indicated as P6, N7, N1, and T7.

(B) Schematic representation of the breeding protocol used to generate +/+ and *p2ry6* (flox/flox);cre/+ mice. *P2ry6* (flox/flox) mice on a C57BL/6 x 129 mixed background (dashed line) or on a C57BL/6 background (solid line) were initially mated with cre/cre mice to generate +/+ and *p2ry6* (flox/flox);cre/+ strains.

(C) PCR amplification products of the wild-type ($p2ry6^{WT}$) and floxed ($p2ry6^{flox}$) p2ry6 gene and of the Cre recombinase in C57BL/6 wild-type (lanes 3-5), *p2ry6* (flox/flox) (lanes 7-9) and

p2ry6 (flox/flox);cre/+ (lanes 11-13) mice, resolved on a 2% agarose gel.

Figure 2. *P*ulmonary inflammation in NaCl- and *Df*-treated +/+ and *p2ry6* (flox/flox);cre/+ mice

(A) Total and differential cell counts from BAL fluid of NaCl-and *Df*-treated +/+ (open bars; n = 9 and 23, respectively) and *p2ry6* (flox/flox);cre/+ (filled bars; n = 9 and 18) mice at the F1 stage of breeding.

(B) Total and differential cell counts from BAL fluid of NaCl-and *Df*-treated C57BL/6 +/+ (open bars; n = 5 and 19, respectively) and *p2ry6* (flox/flox);cre/+ (filled bars; n = 5 and 20) mice at the N10 stage.

(C) Tissue sections of lung showing BVBs from NaCl- and *Df*-treated +/+ and *p2ry6* (flox/flox);cre/+ mice were stained with hematoxylin-azue-2 eosin for assessing inflammatory cell infiltrates (H&E x20) and demonstrating tissue eosinophils (H&E x63, arrow heads) or by PAS reaction for depicting mucus-secreting cells (PAS x20, arrows). Scale bars, 100 (x20) or 25 (x63) μm.

(D) Expression of mRNA transcripts for cytokines and mucus-associated proteins in the lung tissue of NaCl- and Df-treated +/+ (n = 6 and 18, respectively) and *p2ry6* (flox/flox);cre/+ (n = 6 and 15) mice, measured by qPCR. Data are expressed as ratio of the indicated mRNA expression relative to GAPDH mRNA.

Values are mean ± SEM from four (A) and three (B) independent experiments. Pictures in (C) are from one representative mouse per group from one of three independent experiments with similar results. Original magnifications, x20 and x63.

Figure 3. *Df*-induced pulmonary inflammation and PLN cellularity and cytokine release in NaCl- and *Df*-treated C57BL/6 WT and *cre/*+ mice

(A) Total and differential cell counts from BAL fluid of NaCl-and *Df*-treated C57BL/6 WT (open bars; n = 8 and 17, respectively) and cre/+ (filled bars; n = 7 and 18) mice.

(B) Number of cells obtained from PLNs of NaCl- and *Df*-treated C57BL/6 WT and *cre/*+ mice.

(C) Cytokine release from restimulated PLN cells of *Df*-treated C57BL/6 WT and *cre/+* mice.

Values are mean ± SEM from two independent experiments.

Figure 4. Expression of $P2Y_6$ receptors in the lungs, PLNs and spleen

(A) qPCR analysis of $P2Y_6$ receptor mRNA levels in the lungs of NaCl- and *Df*-treated +/+ (open bars; n = 6 and 18, respectively) and *p2ry6* (flox/flox);cre/+ (filled bars; n = 6 and 15) mice.

(B) Immunohistochemical analysis of $P2Y_6$ receptors in the lungs from +/+ and *p2ry6* (flox/flox);cre/+ mice exposed to NaCl and *Df* intranasally. $P2Y_6$ receptor protein, indicated by the brown staining, was detected on cells with the morphology consistent with macrophages (upper left panel, insert) in the lung of +/+ naïve mice and on both macrophages (lower left panel, left insert) and lymphocytes (right insert) in the bronchus-associated lymphoid tissues of +/+ mice. No staining was detected in the lung of NaCl- and *Df*-treated *p2ry6* (flox/flox);cre/+ mice (right panels). Scale bar, 25 μm.

(C) Immunohistochemistry of $P2Y_6$ receptors in PLNs and spleen of NaCl- and *Df*-treated +/+ and *p2ry6* (flox/flox);cre/+ mice. $P2Y_6$ receptors were detected on cells located in paracortical T cell-dependent areas of the organs (arrows), as shown in the inserts at higher magnification. Scale bars, 100 μm.

Values in (A) are mean ± SEM from three independent experiments. Pictures in (B) and (C) are from one representative mouse per group from one of two independent experiments with similar results. Original magnification, x63 (B), x20 and x63 (C).

Figure 5. Cytofluorographic detection of $P2Y_6$ receptors on PLN cell subsets

(A) Dot plots showing the FSC/SSC gated cells and the analysis of the expression of CD4, CD11c, CD8, and B220 on PLN cells from *Df*-treated +/+ mice. Percentages of positive and negative cells are displayed.

(B) Histograms showing the expression of $P2Y_6$ receptors (blue lines) *vs*. isotype control (red lines) on CD4 +, CD8+, and B220+-

gated PLN cells in NaCl- and *Df*-treated +/+ and *p2ry6* (flox/flox);cre/+ mice.

Panels are from one experiment representative of two with similar results.

Figure 6. PLN cellularity and T cell responses

(A) Number of cells obtained from PLNs of NaCl- and *Df*-treated +/+ (open bars; n = 5 and 17, respectively) and *p2ry6* (flox/flox);cre/+ (filled bars; n = 5 and 17) mice.

(B) ELISA measurement of cytokine release from restimulated PLN cells of *Df*-treated +/+ (n = 16) and *p2ry6* (flox/flox);cre/+ (n = 17) mice.

(C) Number of cytokine-producing cells in PLN cells of *Df*-treated +/+ (n = 15) and *p2ry6* (flox/flox);cre/+ (n = 13) mice.

(D) Proliferation (based on CFDA-SE dilution) of CD4+-gated PLN cells from NaCl- and *Df*-treated +/+ and *p2ry6* (flox/flox);cre/+ mice cultured with plate-bound anti-CD3 and soluble anti-CD28 antibodies. The FSC/SSC and CD4/SSC dot plots shown in the figure represent data from *Df*-treated +/+ mice.

Values in (A), (B), and (C) are mean ± SEM from three independent experiments. Panels in (D) are from one representative mouse per group from one of two independent experiments with similar results. The mean data are presented in the text.

Figure 7. Immunoglobulin levels in serum of NaCl- and *Df*-treated +/+ and *p2ry6* (flox/flox);cre/+ mice

(A) Total IgE and (B) *Df*-specific IgG_1 in serum of NaCl- and *Df*-treated +/+ (open bars; n = 10 and 20, respectively) and *p2ry6* (flox/flox);cre/+ (filled bars; n = 11 and 17) mice were measured by ELISA. Values are mean ± SEM from four independent experiments.

Figure 8. Characterization of interstitial macrophages enriched from lungs of *Df*-treated +/+ and *p2ry6* (flox/flox);cre/+ mice

(A) Diff-quick staining of a preparation of lung interstitial macrophages from *Df* +/+ treated mice.

(B) Cytofluorographic characterization of interstitial macrophages obtained from the lung of *Df*-treated +/+ and *p2ry6* (flox/flox);cre/+

mice. The dot plots show the gated populations based on FSC and SSC values and the expression of CD68 and CD11c on the gated cells. The histograms show the expression of MHC-II (blue lines) *vs*. the isotype control (red lines) on the CD68+ cells.

(C) Confocal microscopy analysis of $P2Y_6$ receptor expression on lung interstitial macrophages obtained from NaCl- and *Df*-treated +/+ and *p2ry6* (flox/flox);cre/+ mice.

Pictures in (A) and (C) are from one mouse per group from one of four independent experiments. Panels in (B) are from one experiment representative of two with similar results.

Figure 9. Cytokine release from restimulated cocultures of CD4+ T cells and lung macrophages

Lung macrophages from NaCl- and *Df*-treated +/+ and *p2ry6* (flox/flox);cre/+ mice were co-cultured with CD4+ T cells from +/+ (open bars) and *p2ry6* (flox/flox);cre/+ (filled bars) mice treated with NaCl (left panels) or *Df* (right panels). Values are from one experiment representative of three with similar results.

Figure 1

A
P6
5'
Vector sequence
Exon 2
LA
loxP sites
N7
Neo
Exon 3
N1
SA
3'
T7
Vector sequence
B
C57BL/6
129 / C57BL/6 p2ry6 (flox/+)
C57BL/6 rosa26CreER(T2)
x9
N10 C57BL/6 p2ry6 (flox/+)
cre/cre
p2ry6 (flox/flox)
p2ry6 (flox/flox);cre/+
p2ry6 (flox/flox)
p2ry6 (flox/flox);cre/+
p2ry6WT
p2ry6flox
Cre recombinase
C
1000 bp
500 bp
Ladder
p2ry6WT
p2ry6flox
Cre rec.
p2ry6WT
p2ry6flox
Cre rec.
1 2 3 4 5 6 7 8 9 10 11 12 13
C57BL/6 WT
p2ry6 (flox/flox)
p2ry6 (flox/flox); cre/+

Figure 2

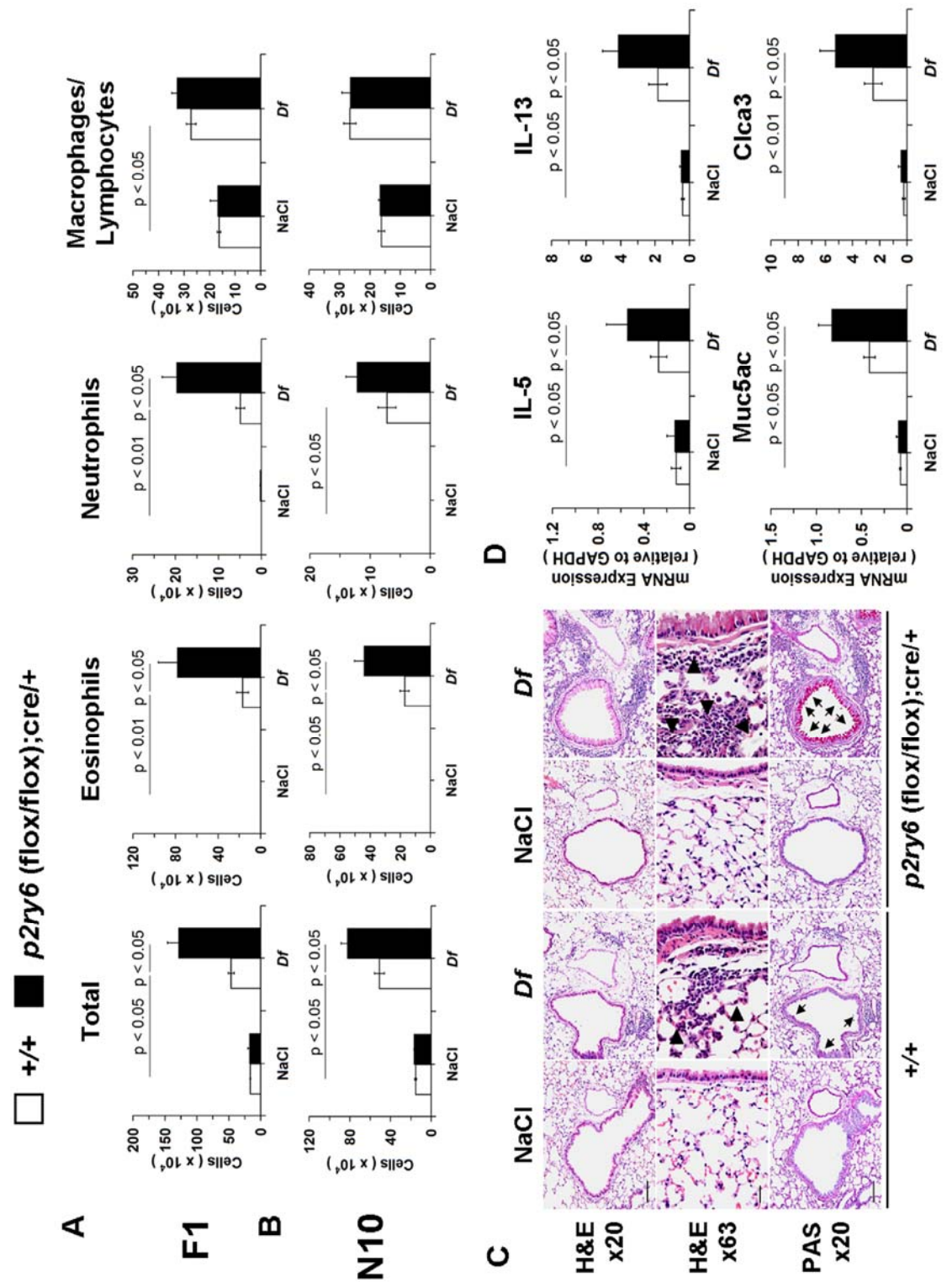
+/+
p2ry6 (flox/flox);cre/+
A
Total
Eosinophils
Neutrophils
Macrophages/ Lymphocytes
F1
B
N10
Cells (x 10⁴)
p < 0.05
p < 0.01
NaCl
Df
C
H&E x20
H&E x63
PAS x20
D
IL-5
IL-13
Muc5ac
Clca3
mRNA Expression (relative to GAPDH)

Figure 3

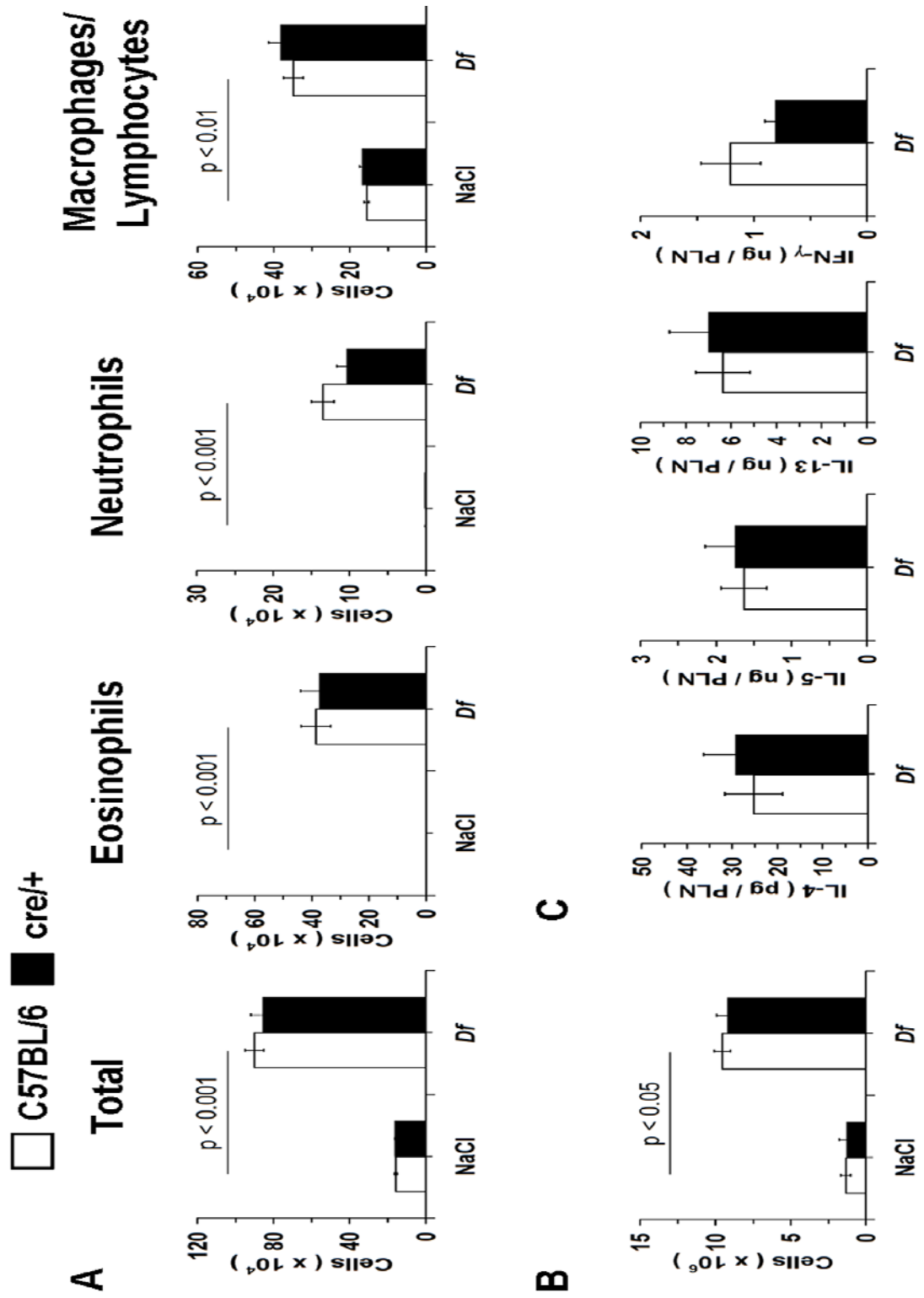
C57BL/6
cre/+
A
Total
Eosinophils
Neutrophils
Macrophages/
Lymphocytes
Cells (x 10⁴)
p < 0.001
p < 0.001
p < 0.001
p < 0.01
NaCl
Df
B
Cells (x 10⁶)
p < 0.05
C
IL-4 (pg / PLN)
IL-5 (ng / PLN)
IL-13 (ng / PLN)
IFNγ (ng / PLN)

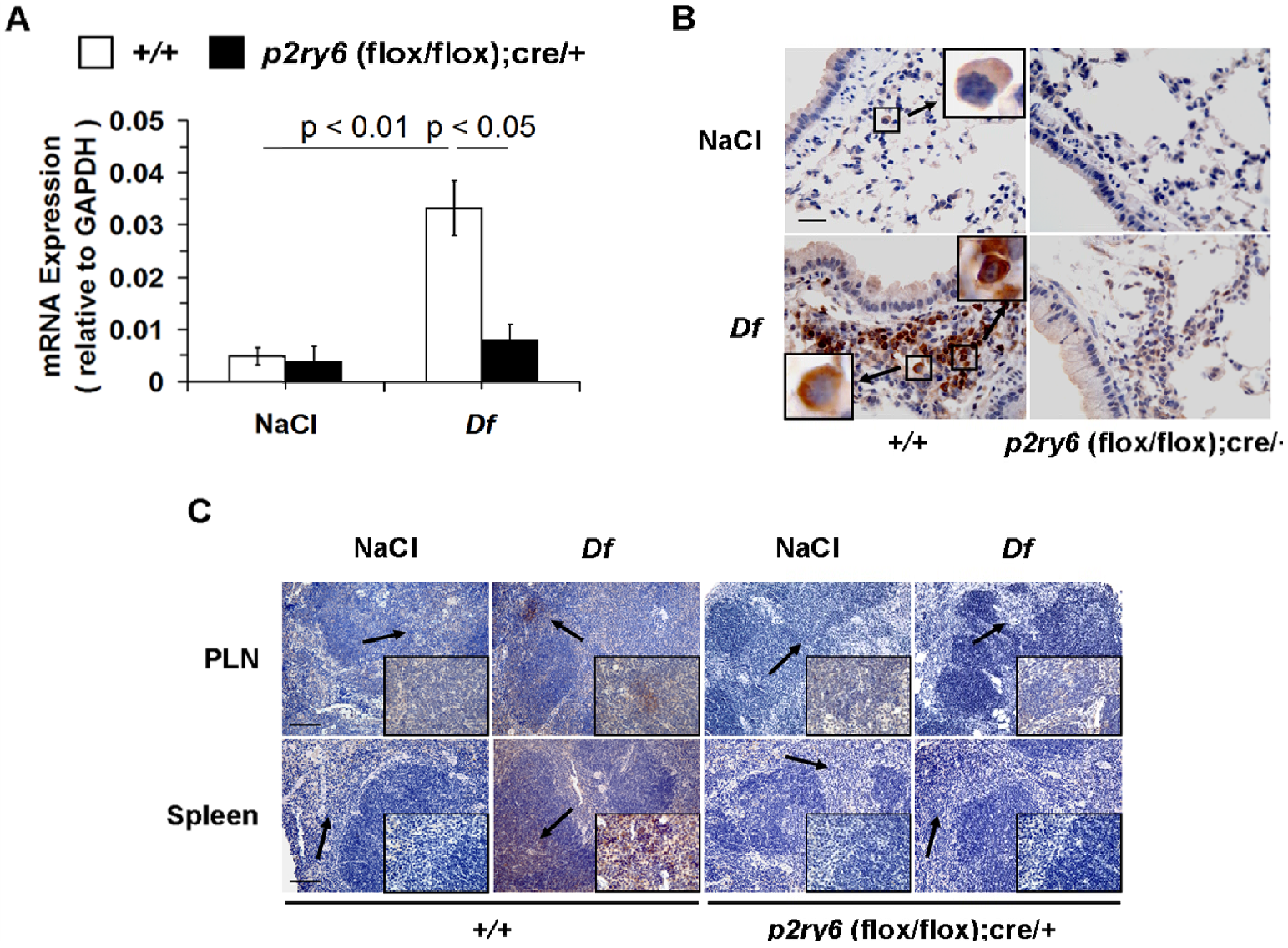
A
+/+
p2ry6 (flox/flox);cre/+
p < 0.01
p < 0.05
mRNA Expression
(relative to GAPDH)
0.05
0.04
0.03
0.02
0.01
0
NaCl
Df
B
NaCl
Df
+/+
p2ry6 (flox/flox);cre/+
C
NaCl
Df
NaCl
Df
PLN
Spleen
+/+
p2ry6 (flox/flox);cre/+

Figure 4

Figure 5

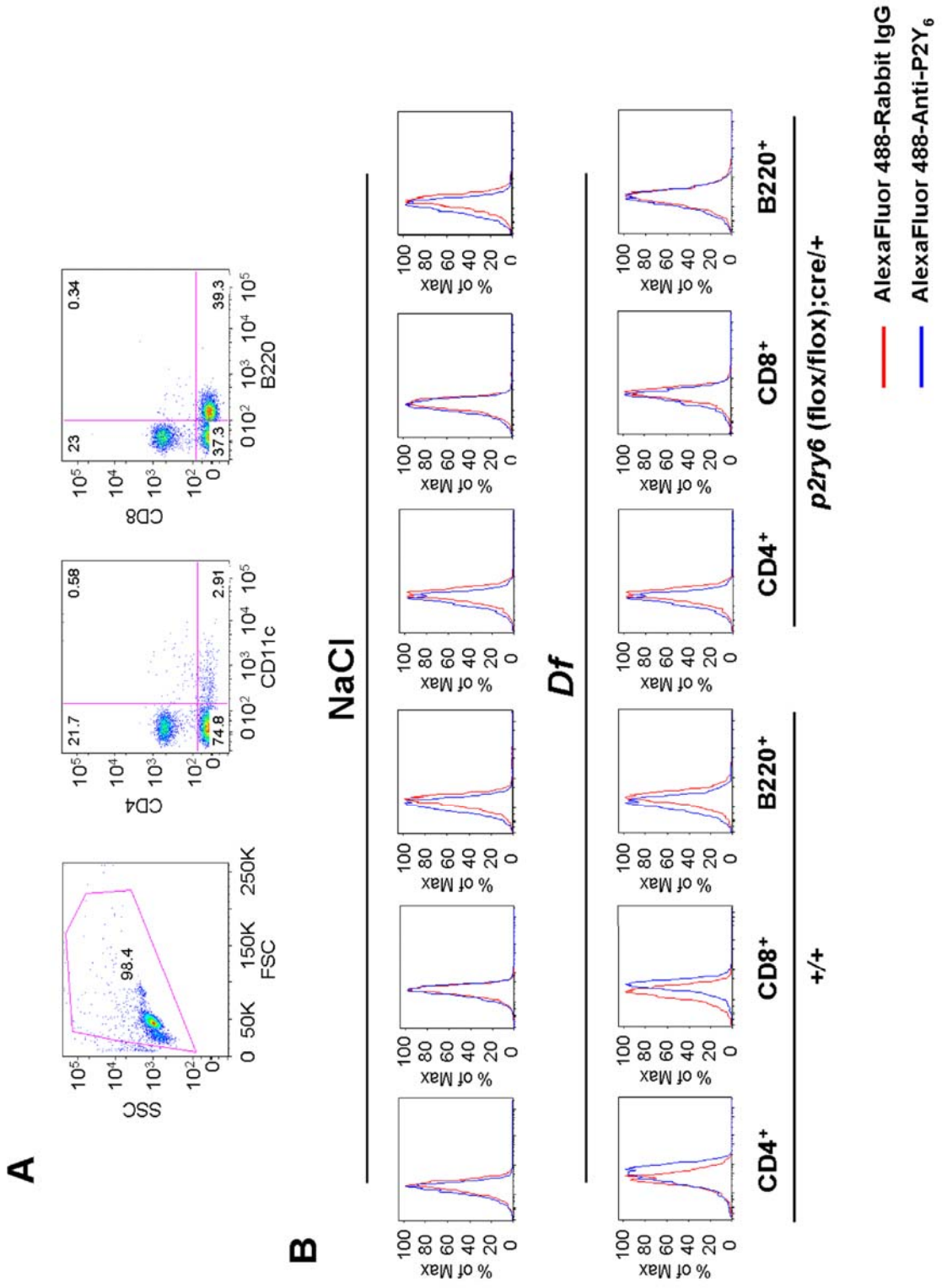
A
SSC
FSC
98.4
CD4
CD11c
21.7
0.58
74.8
2.91
CD8
B220
23
0.34
37.3
39.3
B
NaCl
Df
CD4+
CD8+
B220+
+/+
p2ry6 (flox/flox);cre/+
% of Max
AlexaFluor 488-Rabbit IgG
AlexaFluor 488-Anti-P2Y6

Figure 6

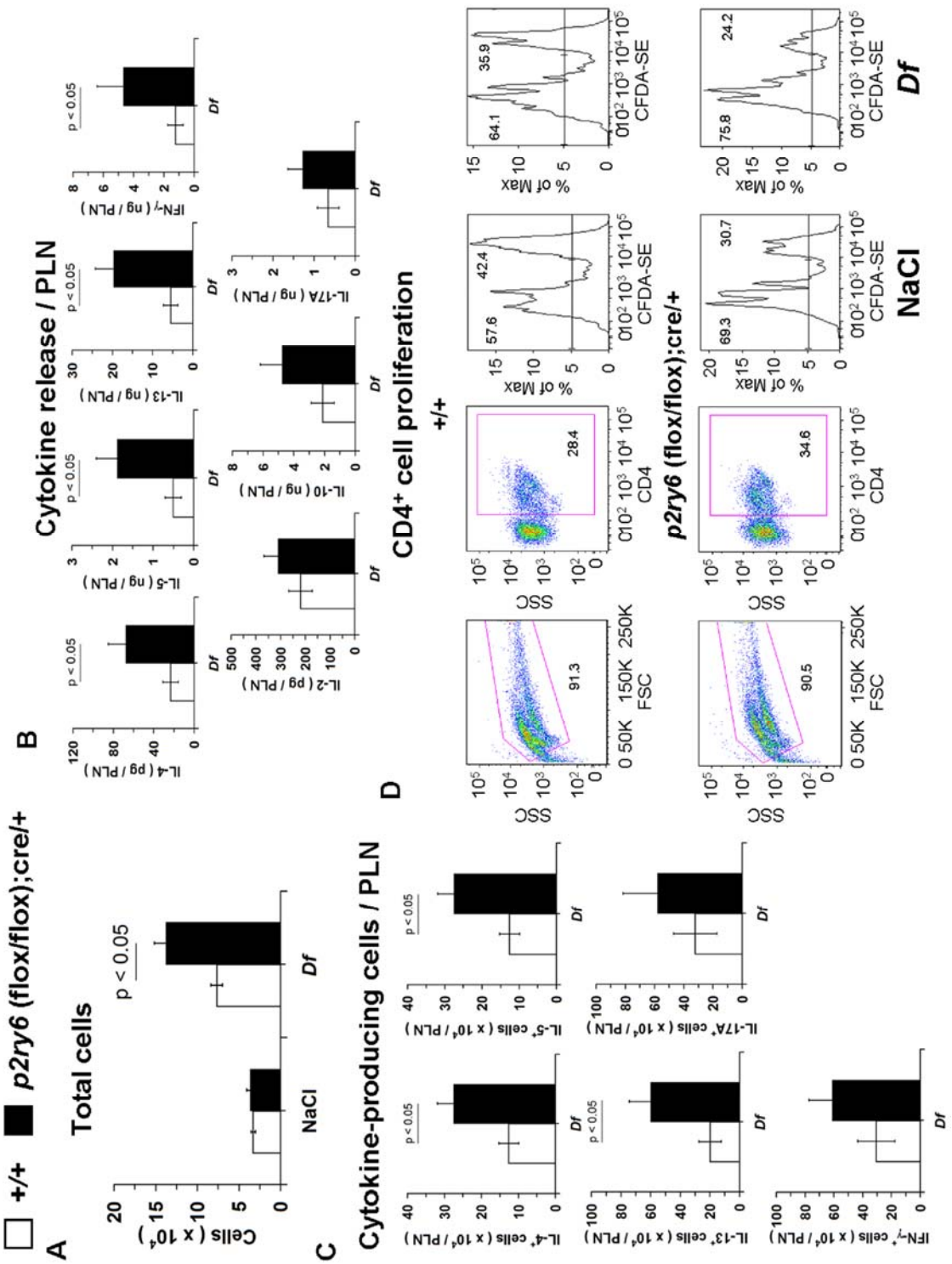
+/+
p2ry6 (flox/flox);cre/+
A
Total cells
Cells (x 10⁴)
p < 0.05
NaCl
Df
B
Cytokine release / PLN
IL-4 (pg / PLN)
IL-5 (ng / PLN)
IL-13 (ng / PLN)
IFN-γ (ng / PLN)
IL-2 (pg / PLN)
IL-10 (ng / PLN)
IL-17A (ng / PLN)
C
Cytokine-producing cells / PLN
IL-4⁺ cells (x 10⁴ / PLN)
IL-5⁺ cells (x 10⁴ / PLN)
IL-13⁺ cells (x 10⁴ / PLN)
IL-17A⁺ cells (x 10⁴ / PLN)
IFN-γ⁺ cells (x 10⁴ / PLN)
D
CD4⁺ cell proliferation
+/+
p2ry6 (flox/flox);cre/+
SSC
FSC
CD4
CFDA-SE
% of Max
91.3
28.4
57.6
42.4
64.1
35.9
90.5
34.6
69.3
30.7
75.8
24.2
NaCl
Df

Figure 7

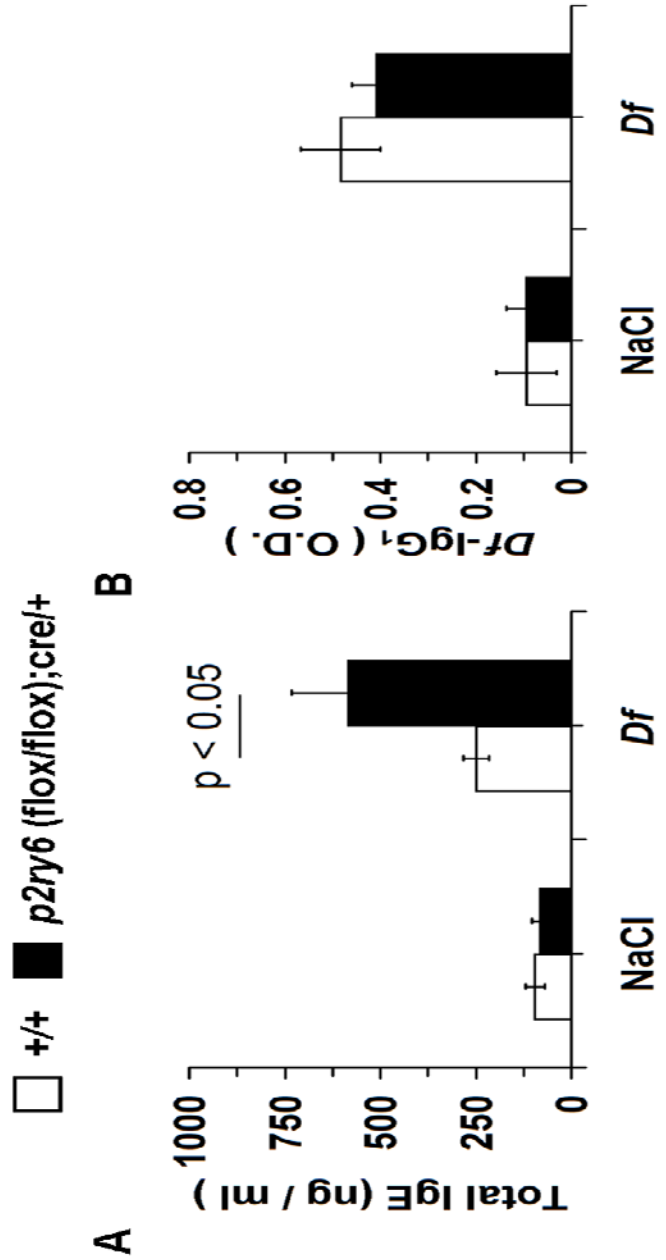
A
B
+/+
p2ry6 (flox/flox);cre/+
Total IgE (ng / ml)
1000
750
500
250
0
p < 0.05
NaCl
Df
Df-IgG1 (O.D.)
0.8
0.6
0.4
0.2
0
NaCl
Df

Figure 8

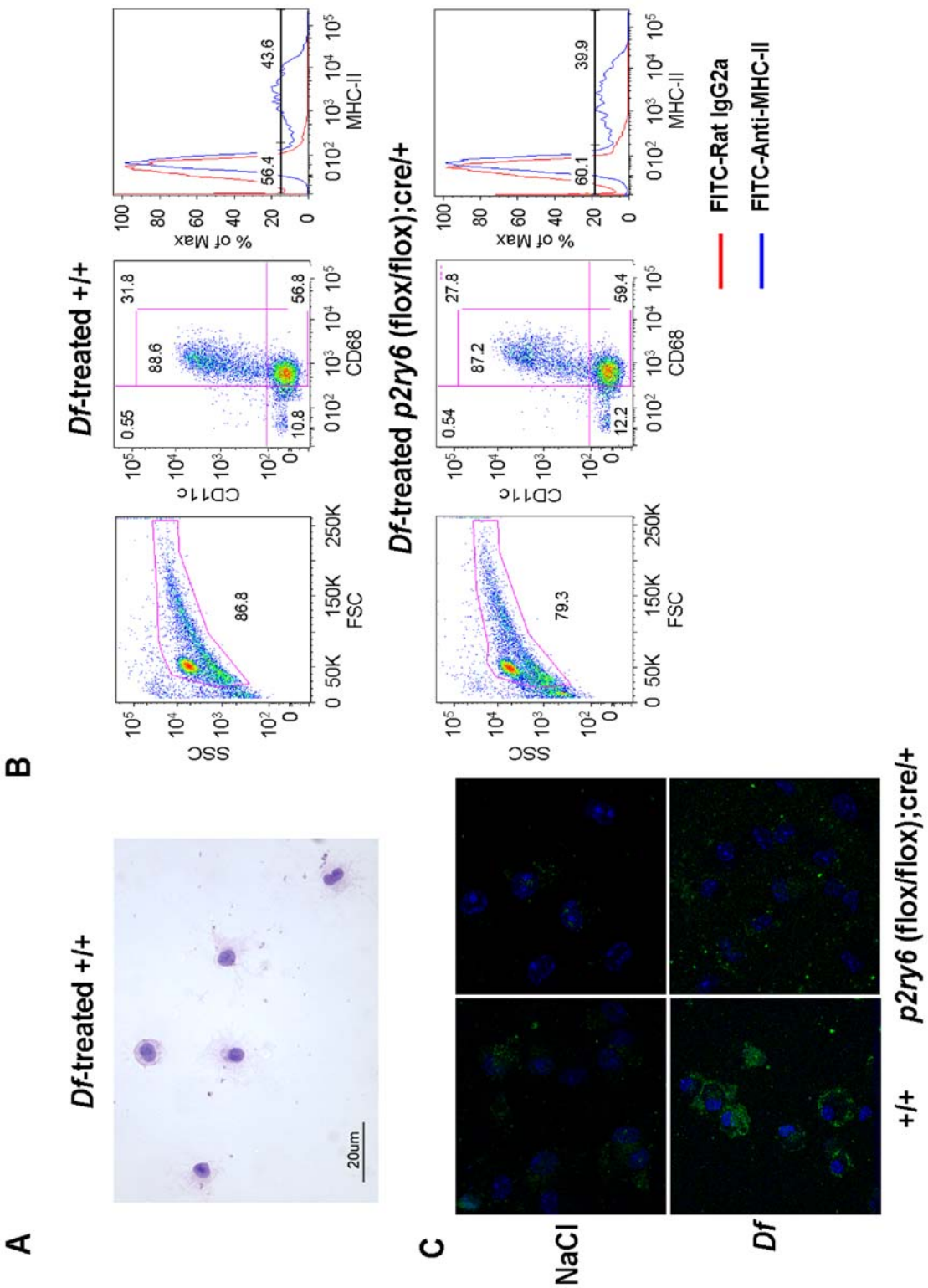
A
Df-treated +/+
20um
B
Df-treated +/+
Df-treated p2ry6 (flox/flox);cre/+
SSC
FSC
CD11c
CD68
MHC-II
% of Max
86.8
79.3
0.55
31.8
88.6
10.8
56.8
56.4
43.6
0.54
27.8
87.2
12.2
59.4
60.1
39.9
FITC-Rat IgG2a
FITC-Anti-MHC-II
C
NaCl
Df
+/+
p2ry6 (flox/flox);cre/+

Figure 9

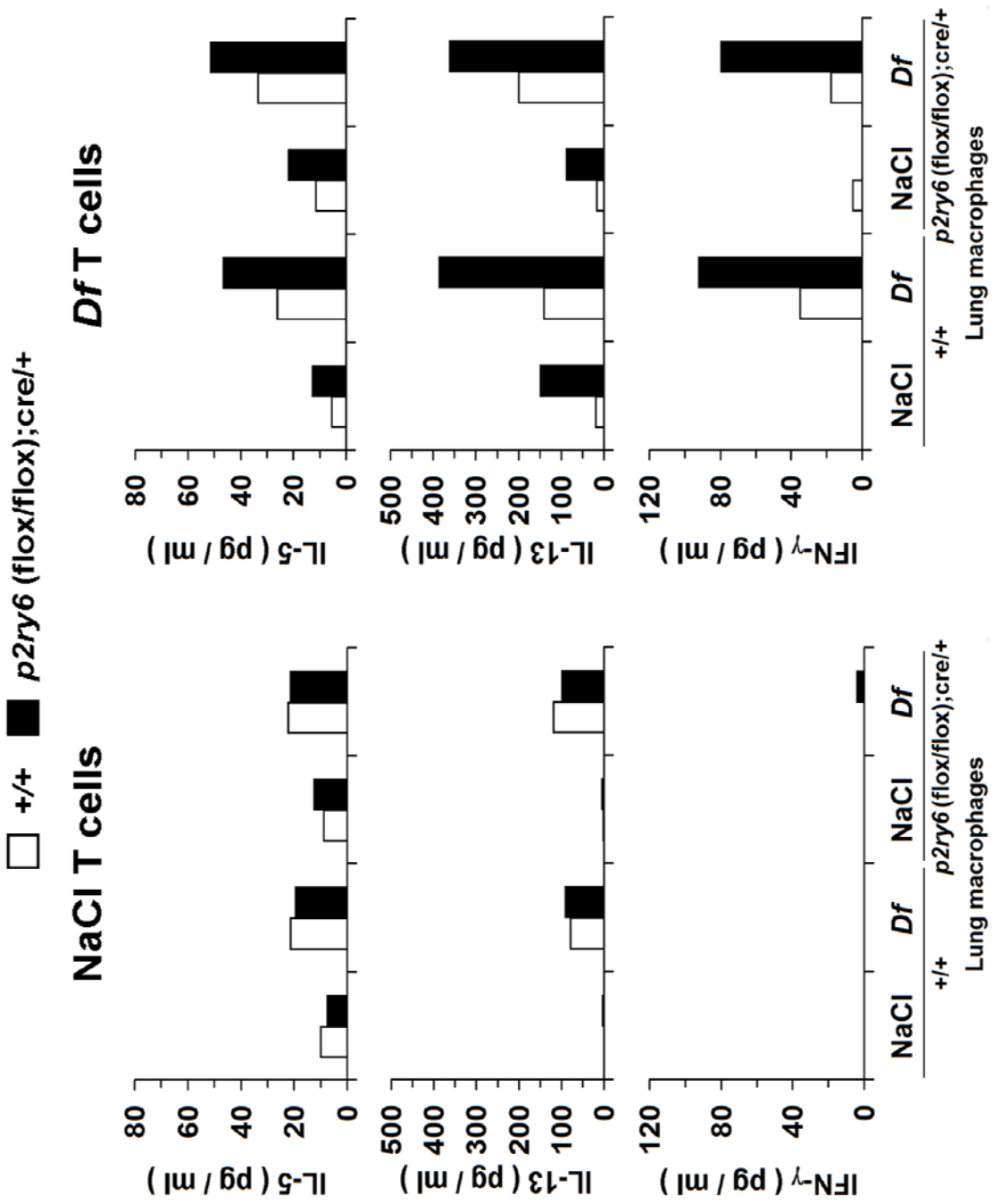
+/+
p2ry6 (flox/flox);cre/+
NaCl T cells
Df T cells
IL-5 (pg / ml)
IL-13 (pg / ml)
IFN-γ (pg / ml)
0
20
40
60
80
100
200
300
400
500
80
120
NaCl
Df
NaCl
Df
+/+
p2ry6 (flox/flox);cre/+
Lung macrophages